

Impact of coal depository and slag disposal from the Plomin thermal power plant on soil composition: insights from geochemical, mineralogical, and organic petrological analyses, Istria, Croatia

Petar Pongrac¹, Tamara Troškot-Čorbić² and Goran Durn^{3,*}

¹ Institute of Earth Sciences, Heidelberg University, Im Neuenheimer Feld 234-236, 69120 Heidelberg, Germany; (petar.pongrac@geow.uni-heidelberg.de);

² INA -Oil Company, Plc., Exploration & Production, Exploration & Upstream portfolio development, Lovinčičeva 4, 10 000 Zagreb, Croatia;

³*University of Zagreb, Faculty of Mining, Geology and Petroleum Engineering, Pierottijeva 6, HR-10000 Zagreb, Croatia;

(*corresponding author: goran.durn@rgn.unizg.hr)

doi: 10.4154/gc.2024.07



Article history:

Manuscript received: January 2, 2024

Revised manuscript accepted: March 21, 2024

Available online: June 21, 2024

Abstract

The potential impact of the open coal depository and the slag disposal of the Plomin thermal power plant (PTPP) on the composition of the surrounding soils was investigated. A comprehensive approach taken included analyses of mineral composition, potentially toxic element content, their bonding properties, distribution to specific geochemical fractions in the soil and investigation of the soil organic petrology and geochemistry. The Cambisols at two sampling sites exhibited a coal dust-covered upper horizon, which led us to consider these soil profiles as Technosol over Cambisol. For practical reasons, we have used the terms Technosol and Cambisol for the upper and lower parts of these profiles respectively. These formations were developed by the long-term deposition of coal dust and slag particles originating from the open coal depository and slag disposal of the PTPP, and widespread wind dispersion. The Technosols, characterized by higher concentrations of lignite and lignite-subbituminous coal, showed elevated levels of C and S. Analysis of the slag sample revealed a mineral composition of mullite, tridymite, graphite, haematite and an amorphous phase, indicating material formation by high temperature coal combustion. The PTPP was identified as the main contributor to the elevated concentrations of Hg, Mo, Se, Sb, U and Cd. The Technosols showed a significant enrichment in Hg, Sb, Se, Mo and U compared to the Cambisols. In the Technosols, elements such as As, Cr, Cu, Fe, Ni and Zn were primarily associated with the organic and Fe-Mn fractions, whereas in the Cambisols these elements, (with the exception of Cu), are mainly associated with the organic and residual fractions. Cadmium, Mn and Pb were predominantly bound to the carbonate and Fe-Mn fractions in all the analyzed samples. The non-residual fraction has been proven to be the predominant repository for As, Zn and Ni in the Technosols and slag, and for Mn, Zn and Cd in the Cambisols. The total content of C and S in the soils and their ratio (C/S) confirmed the higher contamination of soils in the vicinity of the PTPP with coal material. Detection of the coke and soot in the slag sample substantiated its composition as bottom coal ash. In addition, the presence of the bottom coal ash particles in the Cambisol underlined the airborne dispersal of the slag and its integration into the soil composition.

Keywords: Plomin thermal power plant, coal and slag particles, airborne dispersion, potentially toxic elements, soil composition, environmental impact

1. INTRODUCTION

Thermal power plants are one of the largest global sources of pollution. By the combustion of coal in power plants, large amounts of various organic and inorganic pollutants are released, of which the most important are nitrogen and sulfur oxides, carbon dioxide, chlorofluorocarbons (freons), suspended fine-grained material and "heavy metals", referring to potentially toxic elements (SHAMSHAD et al., 2012; KEATING, 2001). Here, all elements that could have a negative environmental impact will be considered as potentially toxic elements.

Istria is the largest peninsula along the Croatian coastline, located in the northwest of the Adriatic Sea. The coal-fired Plomin thermal power plant (PTPP) is situated in the central

part of the eastern coast of the Istrian peninsula, in Plomin Bay (Fig. 1). The main potential source of pollutants in the area are the products of coal combustion in the PTPP. Furthermore, an open coal depository and slag (remain of coal combustion) disposal are situated next to the PTPP (Fig. 2). From these deposits, fine particles of coal dust and ash are easily transported by wind to both nearby land and sea surfaces around Plomin Bay. The different climatic conditions in the individual parts of the peninsula (FILIPČIĆ, 1992; OGRIN, 1995) and the gradual uplift of the carbonate plateau from the south and southwest to the northeast (VELIĆ et al., 1995) largely influenced the diversity of soils on the peninsula. The study area has been exposed to the harmful effects of mining (historical coal and bauxite mining, mining of technical and architectural building stone and brick clay) and constant

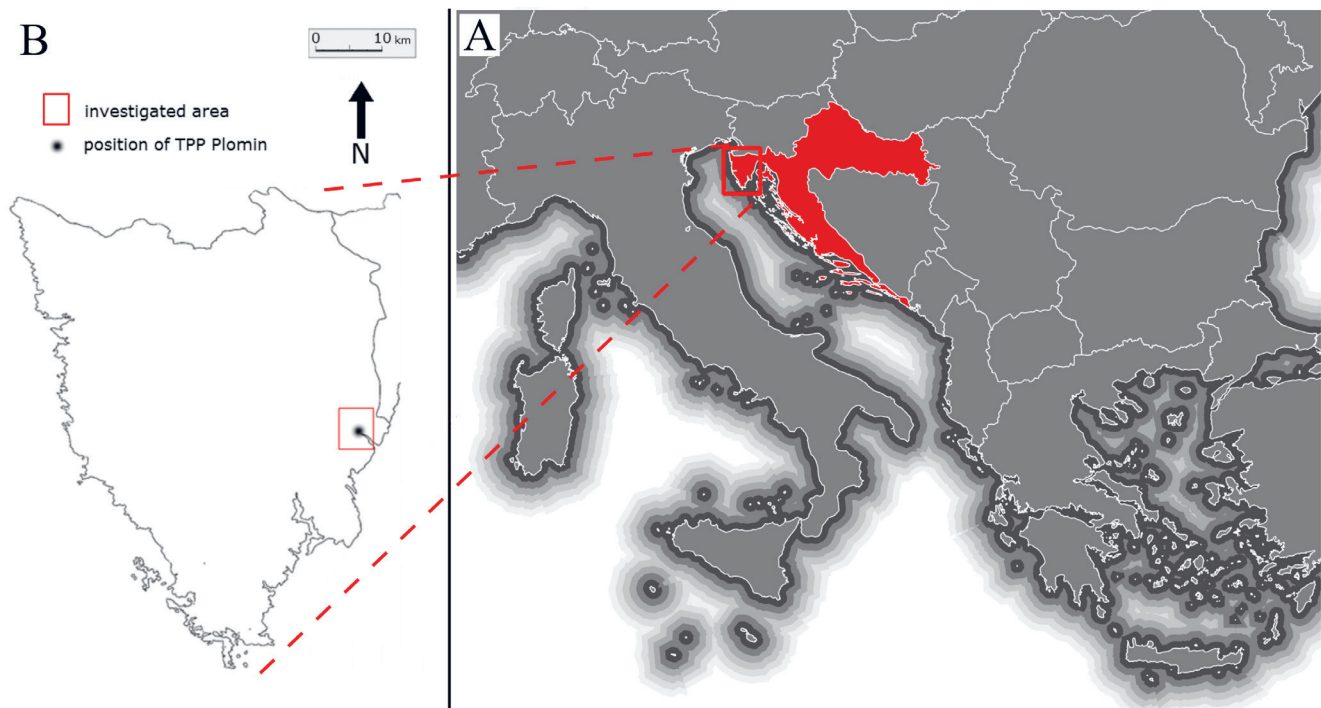


Figure 1. A) Location of Croatia in Europe. B) Location of the Istrian peninsula, study area and the PTPP within Croatia.

contamination with coaly material and coal ash resulting from coal combustion at the PTPP.

Continuous and long-term coal combustion has been proven to largely influence pollution of adjacent soils (e.g., SUN et al., 2010, LI et al., 2014, RODRIGUEZ-IRURETA-GOIENA et al., 2015). MIKO et al., (2003) determined that soils near the Plomin thermal power plant (PTPP) were enriched in Cr, Ni, V, Mn, Cu, Cd and Mo. Relatively high sorption capacity of Fe and Mn oxyhydroxides present in those soils had a crucial role on retention of potentially toxic elements in soil. PROHIĆ & MIKO (1998) compared the concentrations of Se, As, V, Cr, Ni and Zn in the soil in the vicinity of the PTPP with concentrations of the same elements in soils on Risnjak mountain, near the city of Rijeka (Croatia). Concentrations of all these elements except As were significantly higher in soils near the PTPP. Another negative environmental impact of the PTPP is also visible from relatively high levels of pollution of the soils near the PTPP with sulfur, PAHs and the potentially toxic elements Cd and Se, after the continuous combustion of superhigh-organic-sulfur coal (Raša coal), used from 1970 until 2000 (MEDUNIĆ et al., 2016a,b; MALENŠEK et al., 2017). More details on the geochemical characteristics of the Raša coal can be found in MEDUNIĆ et al., (2016b). Water extracts of the most polluted soils and ash samples had shown significant cytotoxic effects on fish cells. Although not statistically significant, the genotoxic effects were also distinct. FIKET et al., (2016) investigated the influence of the PTPP on the surrounding environment regarding REE concentrations and their normalized counterparts in soil, coal, ash and slag samples. Although the resulting REE concentrations in soils near the PTPP were not of concern, soil samples closer to the PTPP showed elevated REE concentrations compared to samples from further away, clearly indicating a negative impact on the environment.

PETROVIĆ et al. (2023) investigated coal combustion residue (coal ash) landfill situated in Štrmac, Istria, near the PTPP. This coal ash is a residue from the local Raša coal. It was found that the landfill is characterized by both 2nd and 3rd stages of coal ash landfill evolution.

The aim of this study was to evaluate and interpret the possible impact of the open coal depository and slag disposal of the PTPP on the composition of the adjacent soils. For this purpose, we conducted a thorough investigation of the mineral composition, content of potentially toxic elements and their bonding and distribution via certain geochemical fractions in the soils, and the organic petrology-geochemistry. The results have provided a detailed background in relation to the coaly material. Within the additional micromorphological study of the soils, we investigated the influence of coal/slag particle deposition on the internal morphology of the soils.

2. MATERIALS AND METHODS

2.1. Field work

The sampling was carried out in the spring of 2013, at five locations around the PTPP (Figs. 2 and 3). Seven soil samples and a sample of the slag from the open disposal next to the PTPP were collected.

Soil sampling and characterization were done in accordance with FAO (2006). At location P1 (Fig. 3-A), the soil profile was open to a depth of 30 cm, and the soil samples were taken from the dark coloured surface horizon (sample P1-A; depth range 0-20 cm) and from depth range 20-30 cm (sample P1-B) (Fig. 3-B). Location P2 (Fig. 3-C), where two samples were taken (0-40 and 40-80 cm respectively), is 300 m west of the PTPP, at almost twice the altitude of location P1. The upper part of the soil profile differed from the lower part by its distinctly darker colour and characteristic bituminous

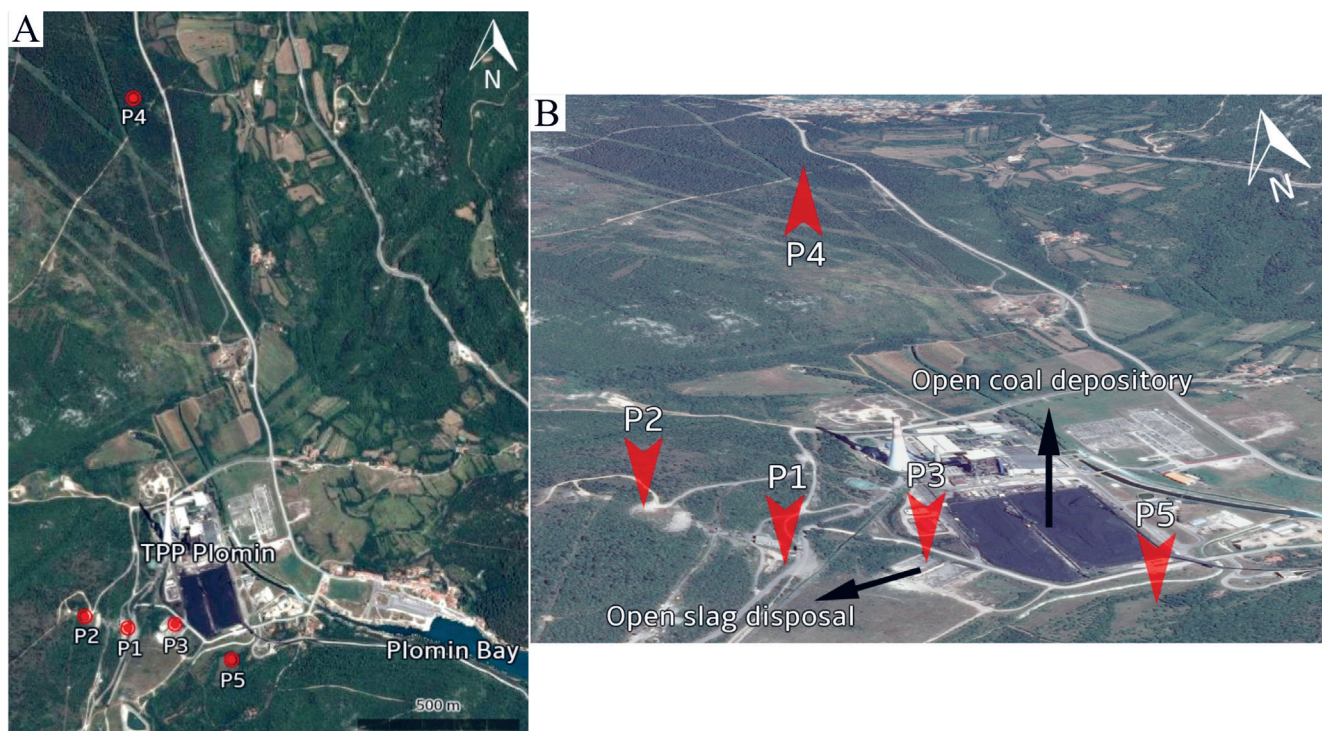


Figure 2. Satellite images of the region surrounding the PTPP showing the sampling locations and the open coal depository and slag disposal locations (Source: Google Earth; 2016).

smell (Fig. 3-D). Location P3 (Fig. 3-E and F) was at the open disposal of slag material, situated next to the PTPP, from where the sample of slag was collected (sample P3). The farthest location P4 (Fig. 3-G) was situated in coniferous forest, from where a sample of the surface soil horizon (sample P4) was taken. At location P5 (Fig. 3-H), (located near to the PTPP in the south), an open soil profile 35 cm deep provided undisturbed samples from a depth range 4-12 cm and 19-28

cm, using Kubienna boxes. All the investigated soil profiles were situated on the carbonate bedrock (nummulitic limestones).

2.2. Laboratory methods

For the purposes of laboratory examinations, a portion of each disturbed soil sample was crushed and sieved through a 2 mm sieve for chemical and mineralogical analyses. For the X-ray powder diffraction (XRD), the sequential extraction procedure



Figure 3. Sampling locations: A) soil profile P1; B) samples from location P1; C) outcrop of limestone with soil on the top at location P2; D) sample of dark upper horizon at location P2; E) open slag disposal at location P3; F) sampling at location P3; G) surface soil horizon at location P4; H) soil profile P5.

(SEP) and the chemical analysis, sieved samples were then ground to a fine-powder in an agate mill, while granulometric analysis and organic petrology-geochemistry analyses were carried out using sieved samples. From undisturbed samples P5-A and P5-B, taken with the Kubiena boxes, soil thin-sections were made. Those samples were only used for the micromorphological analysis.

The distribution of soil particle sizes was determined using a laser diffractometer Shimadzu SALD 2300 and interpreted according to the FAO (2006). Prior to the analysis, organic matter was removed from the samples using hydrogen peroxide (H₂O₂) as described by TRIBUTH & LAGALY (1986). Sodium hexametaphosphate was used as a decoagulant. The sample of slag (P3) was not subjected to granulometric analysis.

Qualitative phase analysis was performed using X-ray diffraction, with a graphite monochromator and CuK α radiation (diffractometer Philips PW 1830). Both the powdered samples (fraction < 2 mm) and the clay fraction (< 2 μ m) were examined. The < 2 μ m fractions were separated by sedimentation in cylinders and quantitatively obtained after the appropriate settling time. The XRD patterns of the clay fraction were obtained after the following treatments: (a) K-saturation, (b) Mg-saturation, (d) K-saturation and ethylene glycol solvation, (e) Mg-saturation and ethylene glycol solvation, (f) heating for two hours at 300 and 550°C. The clay minerals were determined following the methods of THOREZ (1975), BROWN (1961), BRINDLEY & BROWN (1980), MOORE & REYNOLDS (1997) and WILSON (1987).

The chemical composition of the samples was determined at the commercial ACME Analytical Laboratory, Canada. The major element oxides were determined by ICP-emission spectrometry following a lithium metaborate/tetraborate fusion and diluted nitric acid digestion. Trace element content was determined by the ICP-mass spectrometry following a lithium metaborate/tetraborate fusion and nitric acid digestion (Ba, Co, Cu, Ni, Pb, U, V, Zn) or following digestion in Aqua Regia (As, Cd, Hg, Mo, Se). The lithium borate fusion methods provide total element content while digestion in Aqua Regia provides a near-total content. As part of the analysis, the total amounts of carbon and sulfur were measured by the LECO analyzer (combustion and infrared detection technique).

A sequential extraction procedure was performed in order to assess the main bonding sites of elements in the studied soils, according to a modified sediment leaching scheme (TESSIER et al., 1979; HALL et al., 1996), in five steps of separation: (1) adsorbed/exchangeable fraction (AD), (2) carbonated

(calcareous) fraction (CC); (3) Fe and Mn oxyhydroxides fraction (FEMN); (4) organic fraction and finally (5) the residual fraction (RES). Within this framework, concentrations of As, Cd, Cr, Cu, Fe, Mn, Ni, Pb and Zn were measured by Atomic Absorption Spectrometry (AAS, AAnalyst 700), for each of the aforementioned fractions. All elements except As were measured by the flame technique, while concentrations of As were measured by the hydride technique.

The samples of dark coloured top soil (P1-A and P2-A) and sample of slag were subjected to the RockEval pyrolysis, following ESPITALIE et al., (1985). The analyses were also performed on extracted samples. The extractable organic matter (EOM) of the powdered samples was determined by 36-hour Soxhlet extraction with chloroform. The extractable organic matter concentrate obtained after the HCl/HF/ZnCl₂ treatment of soil was examined microscopically (see SCHWAB, 1990) for all types of sample. The organic matter was examined in transmitted and blue fluorescent light using an Olympus BX51 and Zeiss Axio Imager microscope, respectively. The Leitz MPV3 microscope photometer and the Zeiss Axio Imager microscope equipped with the MSP 210 microscope spectrometry system were used for examination in white reflected light and vitrinite reflectance measurements (oil immersion, 546 nm wavelengths).

The undisturbed sample from depth range 4-12 cm (P5-A) represented a transition from the A-horizon to the Bw-horizon, while sample P5-B from depth range 19-28 cm represents the deeper Bw-horizon. The thin-sections for micromorphological analysis were prepared in the Thomas Beckmann laboratory (Schwülper-Lagesbüttel, Germany). Micromorphological interpretation was done according to BULLOCK et al., (1985) and STOOPS (2003), using the Leica DM/LSP petrographic microscope with plane-polarized (ppl) and cross-polarized light (xpl).

3. RESULTS AND DISCUSSION

Based on the highly generalized FAO-UNESCO Soil Map of Croatia (scale 1:1.000.000 – BOGUNOVIĆ et al., 1998), the investigated soils (Locations P1, P2, P4 and P5) were recognized as Cambisols. At sites P1 and P2, the upper part of the Cambisols was covered with anthropogenic material (coal dust). Due to the assumed and remarkable contamination with coal particles (in terms of color, touch and smell of the soil), we considered these soil profiles as Technosol over Cambisol. However, in the text we will use the terms Technosol and Cambisol for the upper (P1/P2-A) and lower (P1/P2-B) parts of these profiles, respectively. The general morphological char-

Table 1. Morphological characteristics of the investigated soils and slag.

soil profile	location altitude (MASL)	depth (cm)	sample	soil color (Munsell Soil Color Chart, 2000)	soil category
P1	32.1	0-20	P1-A	10YR 2/1	Technosol over Cambisol
		20-30	P1-B	10YR 3/4	
P2	68.6	0-40	P2-A	10YR 2/1	Technosol over Cambisol
		40-80	P2-B	7,5YR 4/4	
P3	6.5	-	P3	GLEYS 3/N	-
P4	87.2	0-15	P4	7,5YR 3/3	Cambisol
P5	15.0	0-6	P5-A (4-12 cm)	5YR 3/4	Cambisol
		6-35	P5-B (19-28cm)	5YR 4/4	

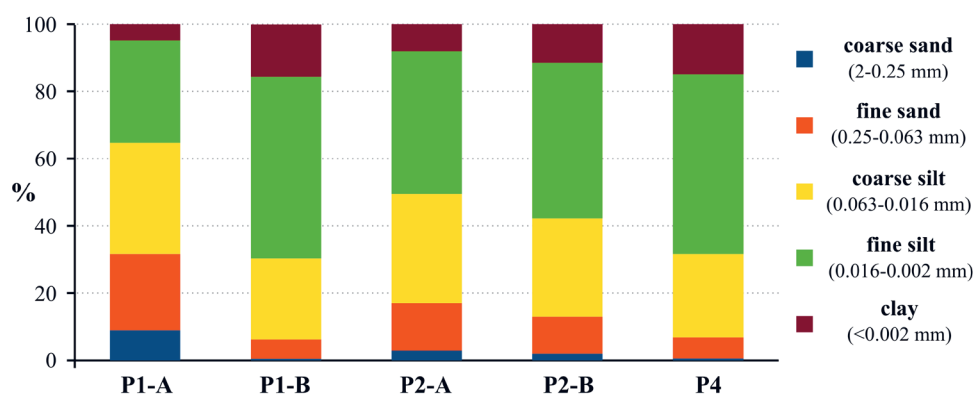


Figure 4. Cumulative granulometric composition of the investigated soil samples (According to FOLK, 1980).

acteristics of the soil profiles are listed in Table 1. Given the broader elevation along sampling sites P1 and P2 together with the fact that the sampling sites are at a higher elevation than the PTPP, it can be assumed that the topography acts as a geomorphological barrier to the most common wind direction from sea to land (approximately E – W; FILIPČIĆ, 1992). This elevated part can therefore easily trap small airborne particles of coal dust that originated from the open disposal areas. In addition, the entire surrounding area probably had a similar barrier effect, as the PTPP is at a notably lower elevation compared to its surrounding. The Technosol layers were therefore most likely formed during years of constant sedimentation of the coal and slag particles.

3.1. Particle size distribution

The analyzed soil profiles were predominantly composed of silt fraction sized particles (Fig. 4). Soil samples P1-A, P2-A and P2-B are more enriched in the sand-sized content compared to samples P1-B and P4. The Technosols (P1-A and P2-A) contain smaller amounts of the clay fraction than the underlying Cambisols.

3.2. Mineral composition

Results of the qualitative mineralogical analysis of the investigated soils are shown in Table 2. Quartz, phyllosilicates, calcite, and haematite were determined in both the Technosols and the Cambisols. Plagioclase, K-feldspar, and goethite were detected only in the Cambisols while the Technosols contain dolomite and a relatively high amount of organic material, as evident from the broad diffuse maximums in the range between 20-30° 2 θ , and the results of RockEval pyrolysis (see section 3.5). The slag sample is composed of quartz, mullite, tridymite, graphite, haematite and an amorphous phase. These latter two mineral assemblage represent an inorganic residue after the combustion of coal (coal combustion products) at high temperatures (WHITE & CASE, 1990; VASSILEV *et al.*, 2003).

The clay fractions of the Technosols and Cambisols are also similar and contain quartz, kaolinite, chlorite and illitic material (Table 3). The mixed-layer clay minerals and vermiculite were detected only at site P2.

3.3. Major element oxides and trace elements

The content of the major element oxides and total sulfur and carbon in the investigated materials is shown in Table 4. The

Table 2. Qualitative mineral composition of soils and slag (fraction < 2 mm).

SAMPLE	Quartz	Plagioclase	K-feldspar	Phyllosilicates	Calcite	Dolomite	Goethite	Haematite	Trydimite, mullite and graphite	AOIC*
P1-A	+			+	+	+		+		+
P1-B	+	+	+	+	+		+	+		
P2-A	+			+	+	+		+		+
P2-B	+	+	+	+	+		+	+		
P3	+							+	+	+
P4	+	+	+	+	+		+	+		

*AOIC – amorphous organic and inorganic compounds

Table 3. Qualitative mineral composition of soils (fraction < 2 μ m).

Sample	Quartz	Kaolinite	Chlorite	Illitic material	Vermiculite	MLM*
P1-A	+	+		+		
P1-B	+	+	+	+		
P2-A	+	+	+	+		+
P2-B	+	+	+	+	+	+
P4	+	+	+	+		

*MLM – mixed layer clay mineral

Technosols contain significantly less SiO₂ compared to the underlying Cambisols. It is similar with the other components, with the exception of CaO, probably due to the slightly higher content of calcite and the presence of dolomite. The lower content of SiO₂ and Al₂O₃ in the Technosols indicates a significantly lower content of phyllosilicates compared to the underlying Cambisols. Technosols have an extremely high sulfur and carbon content compared to the underlying Cambisols, which is direct evidence of the soil contamination with coaly material. Severe pollution of the soils next to the PTPP with sulfur has already been well described in MEDUNIĆ (2016a) and MALENŠEK et al. (2017). Sample P1-B, which was taken closer to the PTPP, contains significantly more carbon and sulfur than sample P2-B, which was farther from the PTPP. The slightly higher carbon value in sample P4 was most likely associated with the organic material from plant residues. This is reflected by a very low S content and a high C/S ratio.

The slag sample consists mainly of SiO₂, Al₂O₃, Fe₂O₃ and carbon (Table 4), which corresponds to its mineral composition (SiO₂ stands for quartz, tridymite and mullite, Al₂O₃ for mullite, Fe₂O₃ for haematite and carbon for graphite; Table 2).

Concentrations of the trace elements are listed in Table 5. In comparison to the Cambisols, the Technosols show enrichment in Hg, Mo, Sb, Se and U, while exhibiting a depletion in As, Ba, Ni, Cd, Co, Cr, Cu and V. The slag contained a high level of Ba. All the aforementioned elements are common potentially toxic elements released during combustion of coal (OVEC, 2009; TOPPIN ORDING, 2009; FUGE, 2005). RODRIGUEZ-IRURETAGOIENA et al. (2015)

found high concentrations of As, Co, Cr, Cu, Fe, Mn, Mo, Pb, Sb, Sn, Tl, V and Zn in some specific areas around the power plant, while LI et al. (2014) determined Cd, Pb, Cu, Zn, Hg, As, and Ni as the most hazardous soil pollutants from coal mining areas. Both of these ranges greatly overlap the range of elements found in this research. The average concentrations of Hg and Mo in the Technosols were almost double the average concentrations in the Cambisols (Table 5). In the case of Hg, all values, with the exception of the slag sample, are significantly higher than the values for the coastal region and the whole of Croatia (Figure 5). The ratio between the average concentration in the Cambisol samples P1-B and P2-B (\bar{x}_B) and the most distant Cambisol sample P4 can be used to estimate the relative release of a particular element from the coal dust. The data indicate an enrichment of Hg in the coal dust, but it is difficult to estimate the release of Hg from the coal and bonding to the soil fractions because the ratio \bar{x}_B/P_4 was < 1. The increased Hg and Mo content in the soil is a consequence of anthropogenic input. The distribution of Se and Sb indicates a similar conclusion. Due to the \bar{x}_B/P_4 ratio of ~ 1 and the higher Sb content in the upper part of the Technosol, the Sb appears to be relatively strongly bound to the coal. The amount and distribution of Se and U also indicate that the coal particles were enriched with Se and U and that their content was higher at shorter distances from the PTPP (Table 5). In addition to the coal dust from the Technosols, the slag sample (P3) also has a relatively high U content, indicating that a large proportion of the U remained in the slag after coal combustion. It is also known that mining and the use of coal in industry and power plants are the main source of

Table 4. Content of major elements oxides in studied samples, including total C and S (wt %).

SAMPLE	SiO ₂	Al ₂ O ₃	Fe ₂ O ₃	MgO	CaO	Na ₂ O	K ₂ O	TiO ₂	P ₂ O ₅	MnO	Cr ₂ O ₃	C	S	LOI*
P1-A	5.61	2.23	1.49	0.83	3.00	0.16	0.21	0.12	0.05	0.02	0.007	63.9	9.14	84.6
P1-B	45.75	16.27	7.21	1.3	1.89	0.45	1.64	0.90	0.16	0.25	0.035	8.04	0.62	23.9
P2-A	7.45	2.93	1.50	0.99	5.64	0.18	0.27	0.16	0.04	0.04	0.008	57.9	8.86	75.8
P2-B	53.10	18.59	7.94	1.66	1.41	0.58	1.83	1.02	0.11	0.24	0.036	1.17	0.05	13.2
P3	56.49	15.16	9.11	1.42	1.97	0.59	1.60	0.68	0.13	0.07	0.016	9.4	0.13	12.5
P4	37.10	14.95	6.34	1.37	2.85	0.34	1.28	0.78	0.22	0.18	0.037	12.2	0.14	34.3

*LOI – loss on ignition

Table 5. Content of trace elements in studied samples (mg/kg; BDL –Below Detection Limit).

ELEMENT	P1-A	P1-B	P2-A	P2-B	P3	P4
As	2.3	18.8	2.7	20.3	1.9	16.4
Ba	90	349	57	381	849	285
Cd	0.8	5.3	1	4.2	BDL	4.9
Co	3.7	29.7	4.3	30	18.2	19.7
Cu	12.3	58.5	11.3	49.4	40.1	35.3
Hg	0.27	0.17	0.35	0.13	0.1	0.22
Mo	4	3.4	3.2	1.5	1.1	1.2
Ni	21.5	83	22.4	92.3	9.6	59.8
Pb	18.5	56.4	18.8	36.9	1.5	62.7
Sb	2.5	0.4	0.8	0.3	0.3	0.3
Se	8.3	5.8	9.1	BDL	BDL	BDL
U	11.7	7.3	6.3	4.1	5.7	3.1
V	84	389	70	359	209	273
Zn	77	89	32	85	26	92

anthropogenic input of toxic uranium into the environment and ecosystems (ATSDR, 1999). Judging from the distribution, the presence of Cd in the studied soils is probably due to the impact of the power plant, although this is not evident from the distribution in the Technosols. This can be explained by the mobility of Cd, as discussed in section 3.4. We consider that Hg, Mo, Sb, Se and U as well as Cd are predominantly of anthropogenic origin and their distribution indicates the negative impacts of the PTPP.

Figure 5 illustrates the variation in concentrations of respective elements obtained through geochemical analysis relative to the statistical values of the same elements'

concentrations for the coastal (Adriatic) part of Croatia and the entire Croatian state, as per the *Geochemical map of the Republic of Croatia* (HALAMIĆ & MIKO, 2009). The concentrations of As, Ba and Ni in the investigated Cambisols are at the level of the median values for the coastal area and the whole of Croatia, while the concentrations of Cd, Co, Cr, Cu, Mn and V are significantly higher. This is particularly true for Cd, which is 5 to 10 times higher compared to the coastal and the whole of Croatia. These results agree with those of MIKO et al. (2003), who found that soils near the PTPP were enriched with Cr, Ni, V, Cu, Cd and Mo, and confirm that anthropogenic pollution is related to the PTPP.

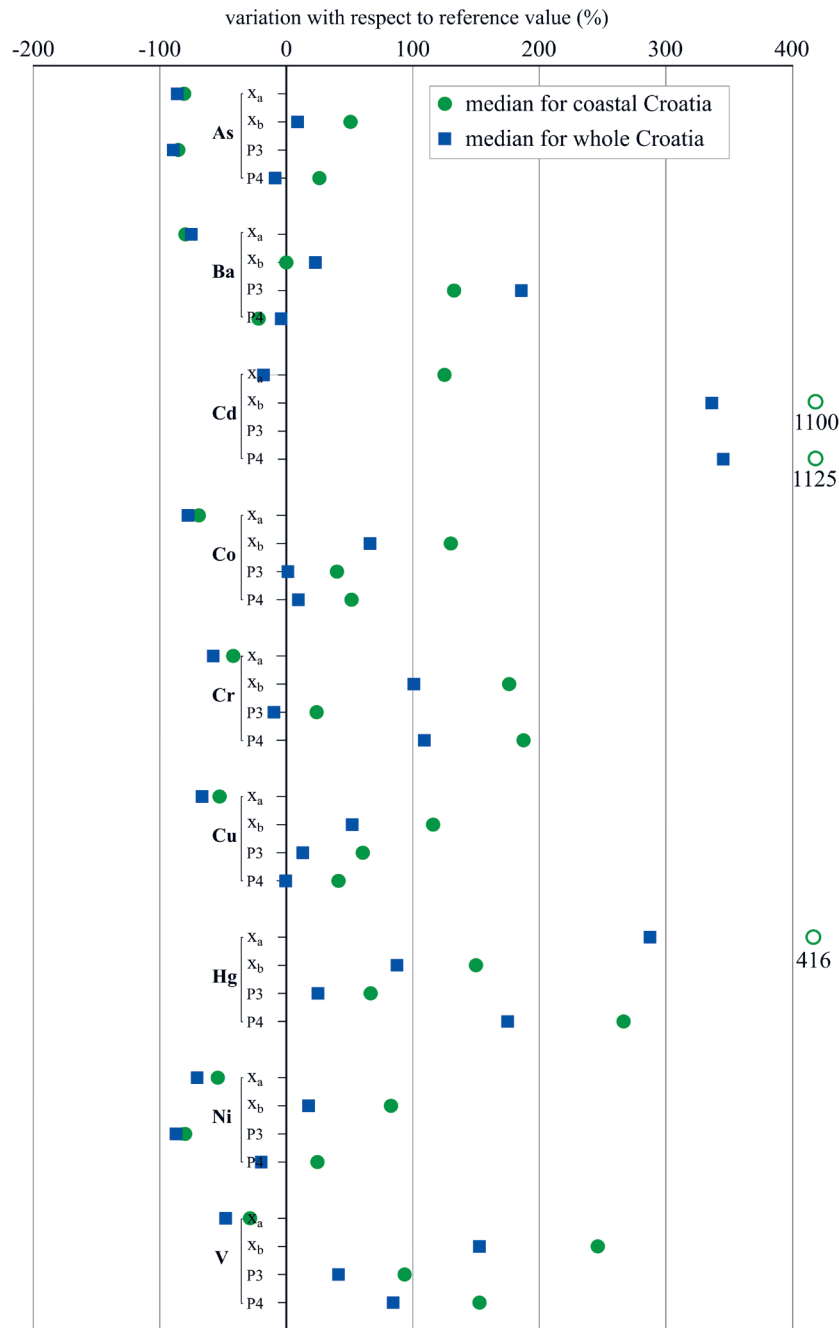


Figure 5. Comparison of the results from geochemical analysis and median values of their concentrations in coastal areas (green circles) and the whole (blue squares) of Croatia according to the Geochemical map of Croatia (HALAMIĆ & MIKO, 2009). Variation of average concentrations from the geochemical analysis relative to the referent values of HALAMIĆ & MIKO, 2009 are presented in %. Results are presented separately for average values of Technosol samples P1-A and P2-A (Xa) and Cambisol samples P1-B and P2-B (Xb), as well as for the slag and the most distant Cambisol sample P3 and P4, respectively. The empty green circles mark the values out of the scale.

3.4. Sequential extraction analysis

By determining the bonding sites of elements in different geochemical fractions of the soil, an interpretation of their behavior and bioavailability can be obtained. This leads to assessment of their environmental risk and possibility of remobilization. Results are shown in Figure 6 and Appendix 1.

The distribution of the analyzed elements among sequential fractions in the Technosols and Cambisols is different for As, Cr, Cu, Fe, Ni and Zn. In the Technosols, these elements are mainly associated with the organic and Fe-Mn fractions, while in the Cambisols, they are mainly bound to the organic and residual fractions (with the exception of Cu). Copper in the

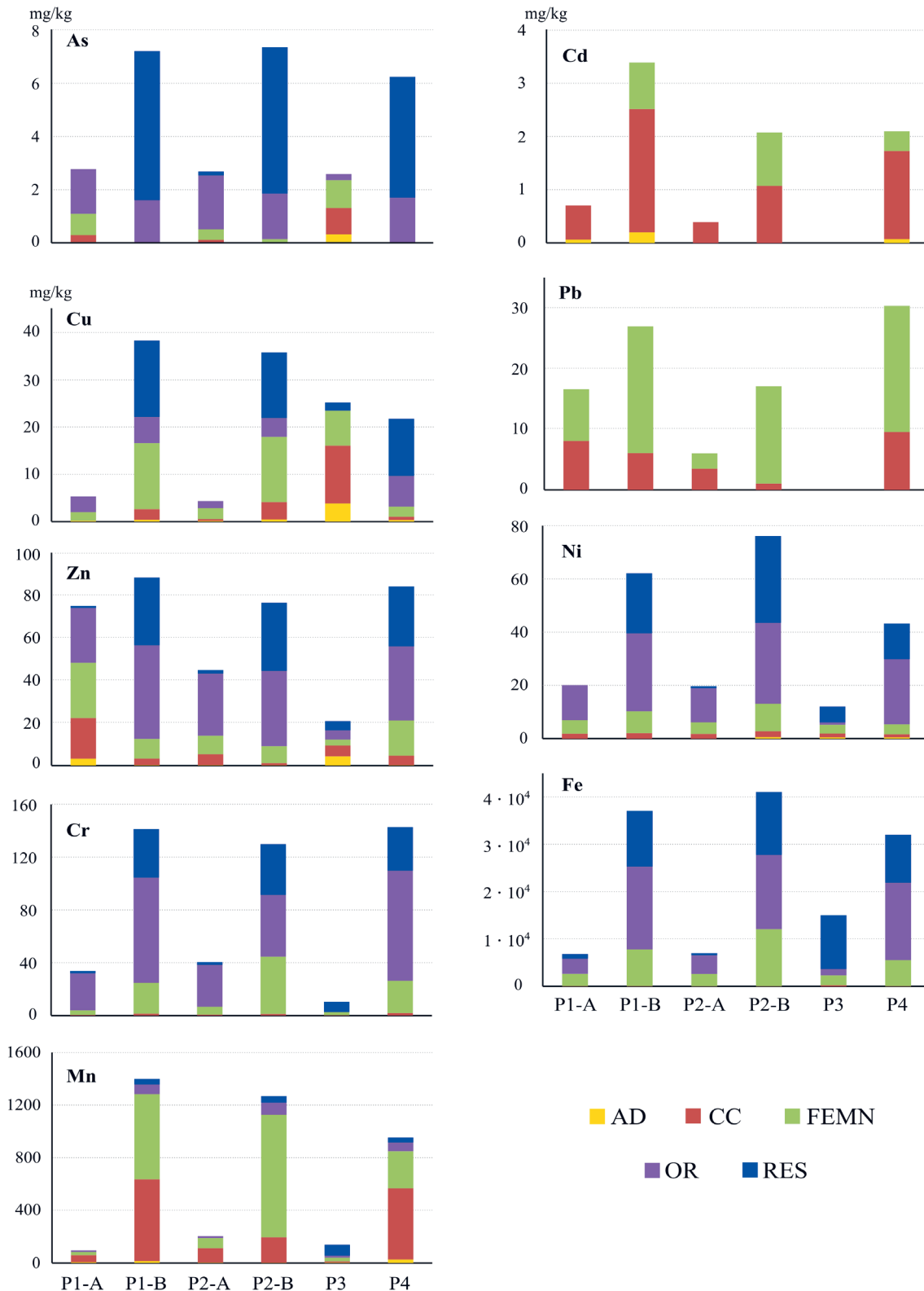


Figure 6. Distribution of the measured elements within sequential extraction fractions of the investigated samples, expressed in mg/kg (see text for explanation of the fractions).

Cambisols is mainly concentrated in the Fe-Mn and residual fractions. Cadmium, Mn and Pb are concentrated in the carbonate and Fe-Mn fractions in all the soil samples. It is important to note that Cd is mainly bound to the carbonate fraction and partly also to the adsorbed/exchangeable fraction. This may explain higher Cd but also Pb values in the Cambisols that are below the Technosols (Table 5). Depending on the relative bioavailability of the elements, Table 6 shows a relationship between (1) the sum of the element concentrations in the first four steps of the sequential extraction (adsorbed, carbonate, Fe-Mn oxyhydroxides and organic fraction) and (2) the total concentration of the element determined by the ICP techniques. The highest ratio (1)/(2) (expressed as a percentage) indicates a relatively higher bioavailability of the element in the soil studied, as this means that a greater proportion of the total content of the element was bound to fractions from which it could be more easily released. Since the bioavailability depends also on many other parameters, this measure is very relative.

Relative bioavailability decreases as follows:

Upper part of Technosols:

Zn = As > Ni > Cr > Mn > Cd > Pb > Fe > Cu

Other soil samples:

Mn > Zn > Cd > Fe > Ni > Pb > Cr > Cu > As

Slag:

As > Zn > Ni > Cu > Mn > Fe > Cr > Cd = Pb.

Distribution of these elements is in a good accordance with the ones estimated by RODRIGUEZ-IRURETAGOIANA et al. (2015) and LI et al. (2014). Unfortunately, we cannot say anything about the bioavailability of Hg, Mo, Sb, Se and U, as we did not have the possibility to perform the sequential extractions for these elements.

3.5. Organic petrology-geochemistry

The results of the RockEval pyrolysis are shown in Table 7. The Technosols (P1-A and P2-A) are extremely rich in organic matter (TOC). Pyrolysis data reveal a high generation potential (S_2) and a high content of free hydrocarbons (S_1) that are still present in samples after extraction. The organic content in the slag sample is also increased, but not with the high range of Technosols.

In Technosols dark and structured fragments with orange-yellowish to brownish fluorescence predominate (Fig. 7 A, B). There was no change in maceral composition in the extracted samples. Structured particles are dominantly represented with the macerals huminite and vitrinite (huminite/vitrinite group) and sporadically with traces of macerals of the inertinite group, fusinite and semifusinite (STACH et al., 1982; TAYLOR et al., 1998). These coaly particles according to the vitrinite reflectance measurements measured on huminite (from 0.35 to 0.40% R_o) belonged to lignite (Fig. 7 C), or lignite A to subbituminous coal C (American terminology), or dull to bright brown coal (German terminology) due to a slightly increased vitrinite reflectance in P2-A sample (0,45 % R_o).

In the maceral composition of the slag particle (P3) structured particles are also predominately huminite (~70% vol). The rest of the composition is represented with macerals of the inertinite group and products of combustion, soot and coke (Fig. 7 D). The vitrinite reflectance of the huminite particles is from 0.3 to 0.4 % R_o . These particles have no fluorescence, except for several cavities. The coke was probably formed by the destructive distillation of lignite at high temperatures. The conditions described were mainly achieved during combustion of lignite at the PTPP, where the coke was disposed of as part of the slag material.

Table 6. Ratio $\times 100$ as a function of relative bioavailability of elements in soils and slag.

SAMPLE	As	Cd	Cr	Cu	Fe	Mn	Ni	Pb	Zn
P1-A	100	87.5	67.06	42.93	56.24	61.44	93.49	89.73	96.1
P1-B	8.58	63.77	43.86	37.78	50.19	70.03	47.67	47.78	63.55
P2-A	94.13	39	70.42	38.41	62.61	65.34	84.51	32.02	100
P2-B	9.12	49.29	37.29	44.21	50.07	65.45	47.12	46.23	52.35
P3	100	0	2.52	58.43	5.69	10.43	63.54	0	63.88
P4	10.36	42.5	43.62	27.39	49.45	65.62	49.88	48.37	60.87

Table 7. RockEval pyrolysis results.

SAMPLE	TOC ^a	S_1 ^b	S_2 ^c	S_3 ^d	T_{max}	S_2/S_3	HI ^e	OI ^f	MINC ^g
	(mass %)	HC (mg) samp. (g)	HC (mg) samp. (g)	CO ₂ (mg) samp. (g)			(°C)	HC (mg) TOC (g)	
P1-A	57.61	19.46	218.96	6.83	418	32.06	380	12	1.78
P1-A _{eks}	52.09	8.03	177.98	6.46	424	27.55	342	12	1.13
P2-A	55.93	20.04	220.92	5.59	421	39.52	395	10	1.81
P2-A _{eks}	52.08	6.59	183.84	5.76	423	31.92	353	11	1.91
P3	3.28	0.14	4.71	0.21	429	22.43	144	6	0.39
P3 _{eks}	5.95	0.33	6.41	1.07	430	5.99	108	18	0.38

^aTOC – total organic carbon

^b S_1 – free hydrocarbons content

^c S_2 – content of hydrocarbons formed during kerogen cracking

^d S_3 – CO₂ amount formed during kerogen cracking

^eHI – hydrogen index

^fOI – oxygen index

^gMINC – mass of inorganic carbon

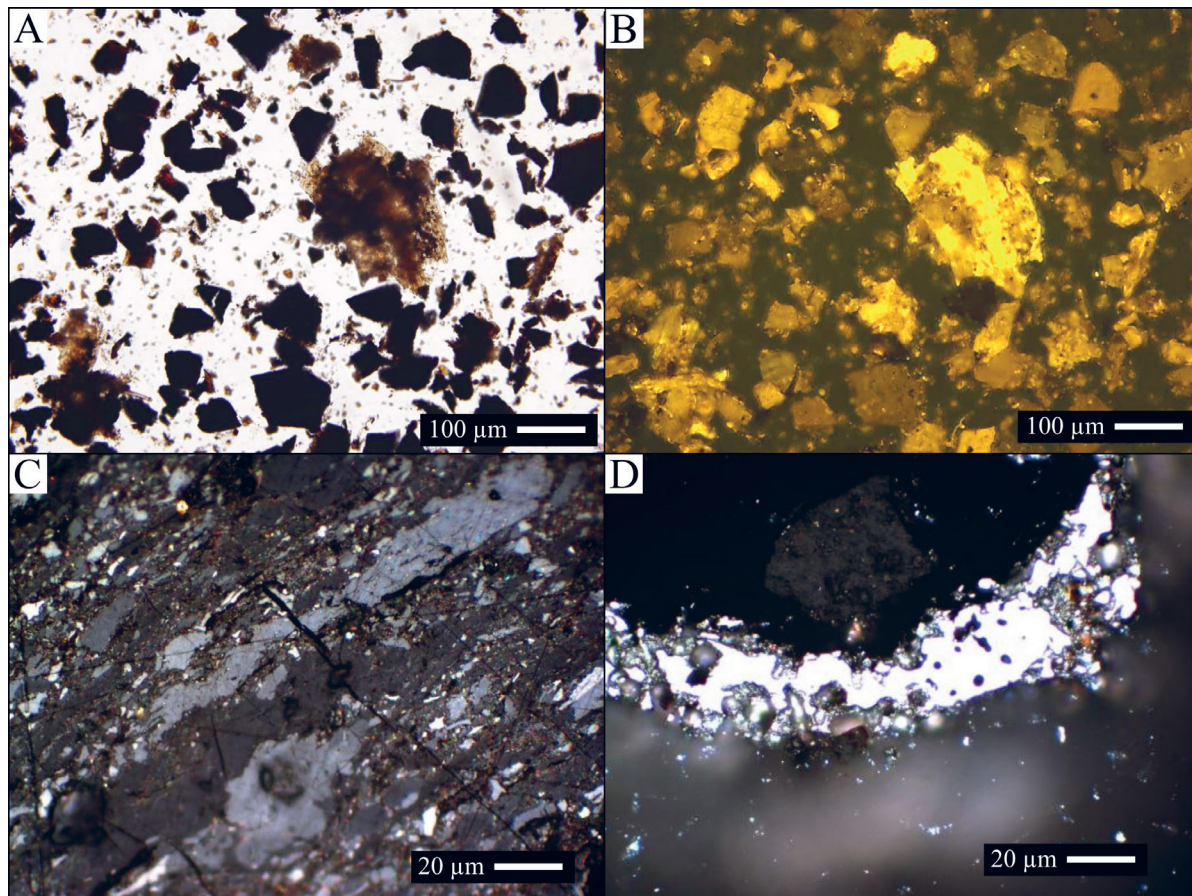


Figure 7. Photomicrographs of A) huminite particles in transmitted light (sample P1-A); B) huminite particles in blue fluorescent light (sample P1-A); C) huminite particle in oil immersion (reflected light; sample P1-A); D) fusinite particle with soot and coke, in oil immersion (reflected light; sample P3).

3.6. Micromorphology

Micromorphological features in both samples from the Cambisol profile (P5) are very similar. The microstructure was granular to vuggy and vuggy/cracked (Fig. 8 A and B), with a moderate to highly developed degree of pedality. The pore space was characterized by irregular cavities and channels. Semi-angular pedorelicts were rarely present (Fig. 8 C), as well as particles of bottom coal ash (Fig. 8 E; cca. 5% vol). The bottom coal ash particles are gray-coloured fragments, ranging up to 6 mm in diameter, containing rounded caverns (Fig. 8 F) which were presumably the result of rapid cooling after combustion. Due to the high content of goethite and subordinate content of haematite (DURN et al., 2001; SINGER et al., 1998), the matrix was brownish-red in colour/ Rounded, branched and irregular iron-oxide impregnative nodules were also observed (Fig. 8 D). The lack of recent and sub-recent clay coatings in the pore spaces of the soil indicates that in the past, the soil was used as farmland (cultivable soil) (DURN, 2003). The presence of bottom coal ash particles in the Cambisol indicates the aerial dispersion of slag and its involvement in the soil composition.

4. CONCLUSION

This research was concerned with the possible influence of the open coal depository and the slag disposal of the Plomin thermal power plant (PTPP) on the composition of the adjacent soils. Since the Cambisols at sites P1 and P2 were covered with

coal dust in the upper part, we considered these soil profiles as Technosols over Cambisols. They were most likely formed by a relatively long-term deposition of coal dust and slag particles from the PTPP. The total C and S content in the soils and their ratio (C/S) confirmed that the soils in the vicinity of the PTPP were highly contaminated with coal and slag material, while the detection of the coke and soot in the slag sample confirmed that the slag consisted of bottom coal ash. The presence of the bottom coal ash particles in the Cambisol samples indicates the airborne dispersion of the slag and its involvement in soil composition. The coal and slag particles were dispersed from the open coal depository and slag disposal, respectively. The Technosols contain particles of lignite and lignite-subbituminous coal, which significantly increased their C and S content. In the slag sample, the mineral association of mullite, tridymite, graphite, haematite and amorphous phases proved that the material was formed by the process of coal combustion at high temperatures. Mercury, Mo, Se, Sb, U and Cd are predominantly of anthropogenic origin and their distribution directly indicates the negative influence of the PTPP. In the Technosols, As, Cr, Cu, Fe, Ni and Zn are mainly bound to organic and Fe-Mn fractions, while in the Cambisols these elements are mainly bound to the organic and residual fractions (with minor variations of Cu), suggesting that it is relatively likely that these elements are mobilized in the Technosols containing comparatively lower amounts of clay minerals and retained in the Cambisols with

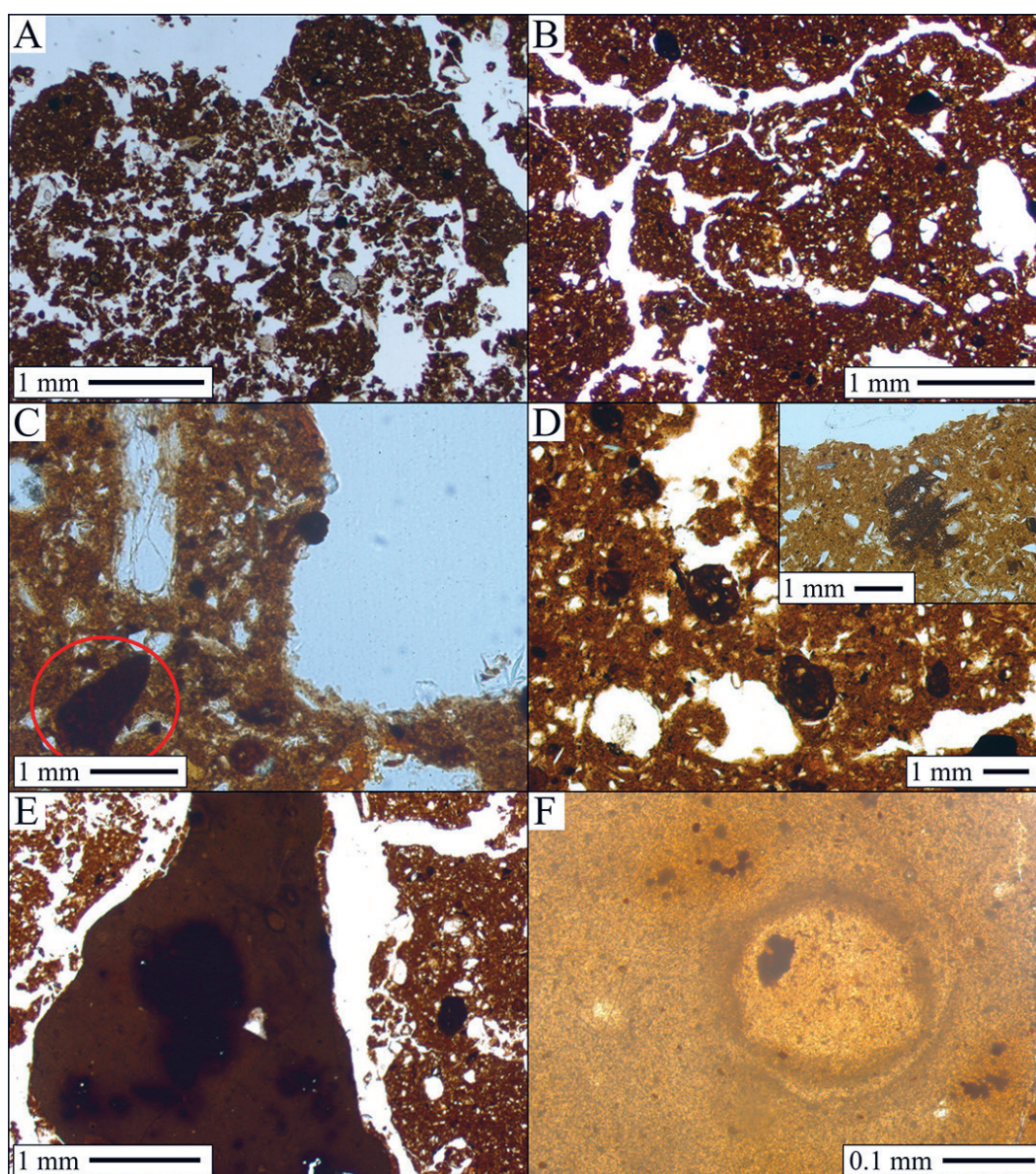


Figure 8. Soil photomicrographs from sample P5-A: **A)** granular to vuggy microstructure; **B)** vuggy/cracked microstructure; **C)** fragment of pedorelict (red circle); **D)** rounded and impregnative (smaller photo) Fe-nodules; **E)** bottom coal ash particle; **F)** cavern on a bottom coal ash particle.

a greater proportion of clay minerals. Cadmium, Mn and Pb are mainly associated with carbonate and Fe-Mn fractions in all the analyzed samples, which increases their potential bio-availability. The non-residual fraction was the most abundant sink for As, Zn, Mn and Ni in the Technosols and for Mn, Zn and Cd in the Cambisols, which is in strong agreement with the results of RODRIGUEZ-IRURETAGOIANA et al. (2015) and LI et al. (2014). The accumulation of these elements in non-residual, especially organic fractions of the Cambisols proves the negative environmental impact of the PTPP and warns of their potential uptake into the ecosystem by vegetation. Further research may investigate the bioavailability of potentially hazardous elements and the likelihood of their uptake into the ecosystem.

ACKNOWLEDGEMENT

This work has been supported in part by the Croatian Science Foundation (project no. IP-2019-04-8054).

REFERENCES

- ATSDR (Agency for Toxic Substances and Disease Registry) (1999): Toxicological Profile for Uranium.– U.S. Department of Health and Human Services, Public Health Service, Agency for Toxic Substances and Disease Registry, Atlanta, GA.
- BOGUNOVIĆ, M., VIDAČEK, Ž., RACZ, Z., HUSNJAK, S., ŠPOLJAR, A. & SRAKA, M. (1998): FAO/UNESCO Croatian soil map, small scale 1:1.000.000.– University of Zagreb, Faculty of Agriculture, project Monitoring Agriculture with Remote Sensing.
- BRINDLEY, G.W. & BROWN, G. (1980): Crystal Structures of Clay Minerals and Their X ray Identification.– Mineralogical Society of Great Britain and Ireland, London. doi: 10.1180/mono-5
- BROWN, G. (1961): The X-ray Identification and Crystal Structures of Clay Minerals.– Mineralogical Society, London
- BULLOCK, P., FEDOROFF, N., JONGERIUS, A., STOOPS, G., TURŠINA, T. & BABEL, U. (1985): Handbook for Soil Thin Section description.– Waine Research, Albrighton, 152 pp.
- DURN, G. (2003): Terra Rossa in the Mediterranean Region: Parent Materials, Composition and Origin.– *Geologia Croatica*, 56/1, 83–100. doi: 10.4154/GC.2003.06

- DURN, G., SLOVENEK, D. & ČOVIĆ, M. (2001): Distribution of Iron and Manganese in Terra Rossa from Istria and its Genetic Implications.– *Geologia Croatica*, Zagreb, 54/1, 27–36. doi: 10.4154/GC.2001.03
- ESPITALIE, J., DEROO, G. & MARQUIS, F. (1985): Rock Eval pyrolysis and its applications.– *Institut Francais du Petrole*.
- FAO (2006): Guidelines for soil description, 4th edition.– FAO, Rome, 97 p.
- FIKET, Ž., MEDUNIĆ, G. & KNIEWALD, G. (2016): Rare earth elements distribution in soil nearby thermal power plant.– *Environ. Earth. Sci.* 75, 598. doi: 10.1007/s12665-016-5410-2
- FILIPČIĆ, A. (1992): Klima Hrvatske.– *Geografski horizonti*, 38/2, 26–35.
- FOLK, R.L. (1980): *Petrology of Sedimentary Rocks*.– Hemphill Publishing, Austin, TX, 182 p.
- FUGE, R. (2005): Anthropogenic Sources.– In: SELINUS O. (ed.): *Essentials of Medical Geology – Impacts of the Natural Environment on Public Health*, British Geological Survey, 43–60.
- HALL, G.E.M., VAIVE, J.E., BEER, R. & HOASHI, M. (1996): Selective leaches revisited, with emphasis on the amorphous Fe oxyhydroxide phase extraction.– *Journal of Geochemical Exploration*, 56/1, 59–78. doi: 10.1016/0375-6742(95)00050-X
- HALAMIĆ, J. & MIKO, S. (ed.) (2009): *Geokemijski atlas Republike Hrvatske (Geochemical map of Republic of Croatia)*.– Hrvatski geološki institut (Croatian Geological Survey), Zagreb, 87 p.
- KEATING, M. (2001): *Cradle to Grave: The Environmental Impacts from Coal*.– Clean Air Task Force, Boston, 8 p.
- LI, Z., MA, Z., VAN DER KUIJP, T.J., YUAN, Z. & HUANG, L. (2014): A review of soil heavy metal pollution from mines in China: pollution and health risk assessment.– *Science of the total environment*, 468, 843–853. doi: 10.1016/j.scitotenv.2013.08.090
- MALENŠEK, N., MEDUNIĆ, G., LOJEN, S., & ZUPANČIĆ, N. (2017): Sulphur isotopes in soil around the thermoelectric power plant Plomin (Croatia).– In: IONETE, R.(ed.): *Book of Abstract: ESIR Isotope Workshop XIV, Băile Govora, Vâlcea*, 133–134.
- MEDUNIĆ, G., AHEL, M., BOŽIČEVIĆ MIHALIĆ, I., GAURINA SRČEK, V., KOPJAR, N., FIKET, Ž., BITUHE, T. & MIKAC, I. (2016a): Toxic airborne S, PAH, and trace element legacy of the superhigh-organic-sulfur Raša coal combustion: Cytotoxicity and genotoxicity assessment of soil and ash.– *Science of the Total Environment* 566–567, p; 306–319
- MEDUNIĆ, G., RAĐENOVIĆ, A., BAJRAMOVIĆ, M., ŠVEC, M. & TOMAC, M. (2016b): Once grand, now forgotten: What do we know about the superhigh-organic-sulfur Raša coal?– *Rudarsko-geološko-naftni zbornik*, 31/3, doi: 10.17794/rgn.2016.3.3
- MIKO, S., DURN, G., ADAMCOVÁ, R., ČOVIĆ, M., DUBÍKOVÁ, M., SKALSKÝ, R., KAPELJ, S. & OTTNER, F. (2003): Heavy metal distribution in karst soils from Croatia and Slovakia.– *Environmental Geology*, 45, 262–272
- MOORE, D.M. & REYNOLDS, R.C. jr. (1997): *X-Ray Diffraction and the Identification and Analysis of Clay Minerals*. 2nd ed.– Oxford University Press, Oxford.
- OGRIN, D. (1995): *Podnebje Slovenske Istre*.– *Annales, Koper*, 381 pp.
- OVEC – OHIO VALLEY ENVIRONMENTAL COALITION (2009): *Heavy Metals Naturally Present in Coal & Coal Sludge*.– Sludge Safety Project.
- PROHIĆ, E. & MIKO, S. (1998): Distribution of selected elements in soils in the vicinity of coal burning power plant "Plomin", Istria, Croatia. *Erdwissenschaftliche Aspekte des Umweltschutzes, Tagungsband*.– In: SAUER, D. (ed): *Österreichisches Forschungs- und Prüfzentrum Arsenal Ges. m. b., Wien*, 319–324.
- Regulations on Agricultural Land Protection against Pollution.– Ministry of Agriculture, Republic of Croatia, 2014. index: NN 9/14
- RODRIGUEZ-IRURETAGOIENA, A., DE VALLEJUELO, S.F.O., GREDILLA, A., RAMOS, C.G., OLIVEIRA, M.L.S., ARANA, G., DE DIEGO, A., MADARIAGA, J.M. & SILVA, L.F.O. (2015): Fate of hazardous elements in agricultural soils surrounding a coal power plant complex from Santa Catarina (Brazil).– *Science of the Total Environment*, 508, 374–382. doi: 10.1016/j.scitotenv.2014.12.015
- SCHWAB, K.W. (1990): Visual kerogen assessment.– In: *Int. Symposium on organic petrology*, Zeist, 10-14.
- SHAMSHAD, A., FULEKAR, M.H. & BHAWANA, P. (2012): Impact of Coal Based Thermal Power Plant on Environment and its Mitigation Measure.– *International Research Journal of Environment Sciences*, 1/4, 60–64.
- SINGER, A., SCHWERTMANN, U. & FRIEDL, J. (1998): Iron Oxide Mineralogy of Terre Rosse and Rendzinas in relation to their moisture and temperature regimes.– *European Journal of Soil Science*, 49, 385–395. Doi: 10.1046/j.1365-2389.1998.4930385.x
- STACH, E., MACKOWSKY, M.T.H., TEICHMÜLLER, M., TAYLOR, G.H., CHANDRA, D. & TEICHMÜLLER, R. (1982): *Coal Petrology*.– Gebrüder Borntraeger, Berlin-Stuttgart, 535 p.
- STOOPS, G. (2003): *Guidelines for Analysis and Description of Soil and Regolith Thin Sections*.– Soil Science Society of America, Inc. Madison, Wisconsin.
- SUN, R., LIU, G., ZHENG, L., & CHOU, C. L. (2010): Geochemistry of trace elements in coals from the Zhuji Mine, Huainan Coalfield, Anhui, China.– *International Journal of Coal Geology*, 81/2, 81–96. doi: 10.1016/j.coal.2009.12.001
- TAYLOR, G.H., TEICHMÜLLER, M., DAVIS, A., DIESSEL, C.F.K., LITTKER, R. & ROBERT, P. (1998): *Organic Petrology*.– Gebrüder Borntraeger, Berlin-Stuttgart, 704 p.
- TESSIER, A., CAMPBELL, P.G.C. & BISSON, M. (1979): Sequential Extraction Procedure for the Speciation of Particulate Trace Metals.– *Analytical Chemistry*, 51/7, 844–851. doi: 10.1021/ac50043a017
- THOREZ, J. (1975): *Phyllosilicates and clay minerals: A laboratory handbook for their X-ray diffraction analysis*.– Editions G. Lelotte, Liege.
- TOPPIN ORDING, E. (2009): *Heavy Metals and Coal: Carbon Footprint Aside, Coal is not Environmentally Friendly*.– Suite 101.
- TRIBUTH, H. & LAGALY, G. (1986): *Aufbereitung und Identifizierung von Boden- und Lagerstättentonen: I. Aufbereitung der Proben im Labor*.– *GIT Fachz. Lab.* 30, 524–529.
- VASSILEV, S.V., MENENDEZ, R., ALVAREZ, D., DIAZ-SOMOANO, M. & MARTINEZ- TARAZONA, M.R. (2003): Phase-mineral and chemical composition of coal fly ashes as a basis for their multicomponent utilization. 1. Characterization of feed coals and fly ashes.– *Fuel*, 82/14, 1793–1811. doi: 10.1016/S0016-2361(03)00123-6
- VELIĆ, I., TIŠLJAR, J., MATIČEC, D. & VLAHOVIĆ, I. (1995): *Opći prikaz geološke građe Istre*.– In: VLAHOVIĆ, I. & VELIĆ, I. (ed-): *Excursion guidebook; First Croatian Geological Congress, Zagreb*, 5–30.
- WHITE, S.C. & CASE, E.D. (1990): Characterization of fly ash from coal-fired power plants.- *J. Mater. Sci.* 25, 5215–5219. doi: 10.1007/BF00580153.
- WILSON, M.J. (1987): *A Handbook of Determinative Methods in Clay Mineralogy*.– Verlag Blackie, Glasgow and London, 308 p.

Appendix 1. Distribution of measured elements within sequential fractions of the soils and slag samples (BDL – below detection limit).

FRACTION	SAMPLE	As (µg/kg)	Cd (mg/kg)	Cr (mg/kg)	Cu (mg/kg)	Fe (mg/kg)	Mn (mg/kg)	Ni (mg/kg)	Pb (mg/kg)	Zn (mg/kg)
AD	P1-A	28.61	0.06	BDL	0.17	3.85	6.21	BDL	BDL	3.21
	P1-B	BDL	0.20	BDL	0.36	1.79	13.55	BDL	BDL	0.21
	P2-A	BDL	BDL	BDL	0.15	1.36	3.15	BDL	BDL	0.17
	P2-B	BDL	BDL	BDL	0.44	0.41	1.28	0.56	BDL	0.11
	P3	324.86	BDL	BDL	3.85	0.00	3.41	0.45	BDL	4.34
	P4	BDL	0.07	BDL	0.31	1.18	26.13	0.44	BDL	0.15
CC	P1-A	263.63	0.64	0.51	0.02	43.24	53.13	1.80	8.05	19.10
	P1-B	BDL	2.31	1.42	2.27	46.80	622.81	2.05	6.06	3.06
	P2-A	111.05	0.39	0.70	0.37	19.44	108.53	1.74	3.47	5.16
	P2-B	BDL	1.07	1.28	3.68	24.35	193.37	2.18	1.02	1.01
	P3	984.59	BDL	0.29	12.17	209.08	8.52	1.42	0.00	5.07
	P4	18.68	1.65	1.84	0.72	32.03	541.33	1.18	9.54	4.53
FEMN	P1-A	802.02	BDL	3.47	1.82	2587	24.10	5.11	8.55	25.98
	P1-B	BDL	0.87	23.35	13.90	7717	646.81	8.22	20.89	9.29
	P2-A	393.60	BDL	5.91	2.32	2595	76.55	4.37	2.55	8.63
	P2-B	142.02	1.00	43.38	13.73	12025	930.67	10.31	16.04	7.95
	P3	1049.71	BDL	2.45	7.41	2071	28.87	3.31	0.00	2.75
	P4	BDL	0.37	24.47	2.11	5473	280.90	3.74	20.79	16.47
OR	P1-A	1683.36	BDL	27.94	3.27	3222	11.79	13.19	BDL	25.71
	P1-B	1613.08	BDL	79.62	5.57	17529	73.59	29.30	BDL	44.00
	P2-A	2038.51	BDL	31.70	1.50	3948	14.32	12.82	BDL	29.26
	P2-B	1709.89	BDL	46.63	3.99	15739.	92.03	30.44	BDL	35.43
	P3	229.10	BDL	0.00	BDL	1342.5	15.77	0.92	BDL	4.45
	P4	1680.26	BDL	83.44	6.53	16406	67.00	24.47	BDL	34.85
RES	P1-A	BDL	BDL	1.77	BDL	930.1	BDL	BDL	BDL	0.92
	P1-B	5598.19	BDL	36.75	16.07	11774	41.02	22.57	BDL	31.80
	P2-A	139.03	BDL	2.15	BDL	431.2	BDL	0.77	BDL	1.57
	P2-B	5503.41	BDL	38.48	13.79	13272	49.75	32.59	BDL	31.92
	P3	BDL	BDL	7.70	1.65	11387	81.49	5.92	BDL	4.25
	P4	4545.32	BDL	32.83	12.01	10104	37.72	13.35	BDL	28.13